THE ANTRONA NAPPE: LITHOSTRATIGRAPHY AND METAMORPHIC EVOLUTION OF OPHIOLITES IN THE ANTRONA VALLEY (PENNINE ALPS)

Fabio Turco and **Paola Tartarotti**✉

Dipartimento di Scienze della Terra, Università degli Studi di Milano, Italy.
✉ *Corresponding author, e-mail: paola.tartarotti@unimi.it.*

Keywords: *Antrona ophiolite, lithostratigraphy, eclogite. Pennine Alps.*

ABSTRACT

The Antrona ophiolite (western Central Alps) represents a tectonic fragment of the oceanic lithosphere of the Upper Jurassic - Lower Cretaceous Ligurian-Piedmont basin, a section of the Western Alpine Tethyan Ocean. The Antrona ophiolite occurs at lower structural levels in the Alpine nappe stack and is sandwiched between the overlying continental Monte Rosa Nappe (upper Penninic) and the underlying Camughera-Moncucco continental Unit (middle Penninic). The Monte Rosa Nappe is overlain by the Zermatt Saas ophiolitic Unit. Despite the tectono-metamorphic reworking, the Antrona ophiolite exhibits all typical lithologies of oceanic lithosphere: ultramafic and mafic plutonic rocks, mafic volcanic rocks and deep-sea sediments can be recognized. Several rock types were distinguished among mafic rocks. New findings and inferences are: i) the occurrence of probable relics of magmatic structures in some amphibolites, inferred to be pillow lavas or pillow breccia; ii) the occurrence of lawsonite pseudomorphs-bearing amphibolites, not described so far in the study area as precursor of the origin of epidote-amphibolites the Antrona Valley. A qualitative P-T diagram deduced from the stability conditions of mineral parageneses is presented and compared with published P-T paths for the Antrona and Zermatt-Saas ophiolites. The metamorphic evolution of the studied rocks is characterized by blueschist prograde path followed by high pressure (eclogitic) metamorphic peak. P-T estimates for the metamorphic peak were calculated by the Na-clinopyroxene garnet equilibria and the jadeite content in omphacite. T = 372°C for a nominal pressure of P = 1 GPa and T = 386°C for a nominal pressure of P = 1.5 Gpa were obtained. Jd_{30} as maximum Jadeite content suggests P > 1 Gpa. Retrograde path, although not well constrained, is dominated by epidote-amphibolite/amphibolite facies conditions, in accord with published data, differing from those inferred so far for the overlying Zermatt-Saas ophiolite.

INTRODUCTION

The Zermatt-Saas and Antrona metaophiolites represent remnants of the oceanic lithosphere of the Mesozoic western Tethys, now dismembered as tectonic slices in the internal Pennine domain of the western Central Alps. The Antrona Unit obtained not much attention in the past, despite its crucial tectonic position within the nappe stack.

This paper presents the results of a geological study carried out on the eastern side of the Antrona Valley, a tributary of the Ossola Valley (western Central Alps). Despite the polyphase metamorphic history, the Antrona ophiolite exhibits all typical lithologies of oceanic lithosphere, i.e., ultramafic and mafic plutonic rocks, mafic volcanic rocks and deep-sea sediments. This work focuses on plutonic and volcanic metabasites. Among the mafic volcanic rocks (commonly described in literature as "amphibolites") several lithologies, often retaining relict magmatic structures, were distinguished. Lozenge-shaped porhyroblasts consisting of epidote+chlorite aggregates were observed for the first time in amphibolites from the study area. They are interpreted as pseudomorphs of former lawsonite, thus providing a clue to discuss the metamorphic evolution of the Antrona ophiolite. Temperature and pressure conditions were estimated for the high pressure metamorphic peak, whereas the prograde and retrograde P-T diagram was deduced from the stability conditions of mineral parageneses.

GEOLOGICAL SETTING

Regional geology

In the Pennine-Lepontine nappe stack (e.g., Escher et al., 1987; 1993), the Zermatt-Saas ophiolite nappe mantles the Monte Rosa Unit and disappears below the Mischabel backfold; the Antrona ophiolite is situated on the footwall of the Monte Rosa Nappe (Fig. 1) and in turn overlays the middle Penninic Camughera-Moncucco Nappe (Bearth, 1956; Laduron, 1976; Bigioggero et al., 1981; Keller et al., 2005b). The Antrona and the Zermatt-Saas metaophiolites almost completely envelop the Monte Rosa Nappe, with the exception of the area between Gornergrat and "Passo della Preja", where the Furgg Zone is dominant and only thin slices of ophiolite rocks are present (Fig. 1).

The Monte Rosa Nappe is a large NW-vergent recumbent anticline, strongly refolded by S-vergent backfolds of supposed Oligocene age (Milnes et al., 1981; Escher et al., 1997; Steck et al., 1997). The Monte Rosa Nappe, together with the Gran Paradiso and Dora Maira "massifs", constitute the inner and upper continental nappe system of the Penninic Zone in the Western Alps. In the Monte Rosa Nappe, two main pre-Alpine protoliths have been recognized: a pre-granitic metamorphic complex (Bearth, 1952; Gosso et al., 1979; Dal Piaz, 1993; Keller and Schmid, 2001; Keller et al., 2005a), consisting of high grade paragneiss rich in mid- to coarse-grained pegmatites, and a granitic complex represented by dominant granitic-granodioritic bodies cut by aplitic and pegmatitic dykes of Late Carboniferous and Permian ages (Hunziker, 1970; Frey et al., 1976). During the Alpine orogeny, the pre-granitic complex has been reworked into garnet micaschists and albitic schists, and the granitic bodies into massive, schistose or mylonitic orthogneiss.

In the study area, the Antrona ophiolite is separated from the Monte Rosa basement by the Furgg Zone (Argand's "synclinal de Furggen", Argand, 1911). The Furgg Zone consists of micaschists, albitic schists, and leucocratic gneisses (Permian-Carboniferous?) with eclogitic to greenschist-facies mafic boudins, thin micaceous quartzites and dolomitic mar-

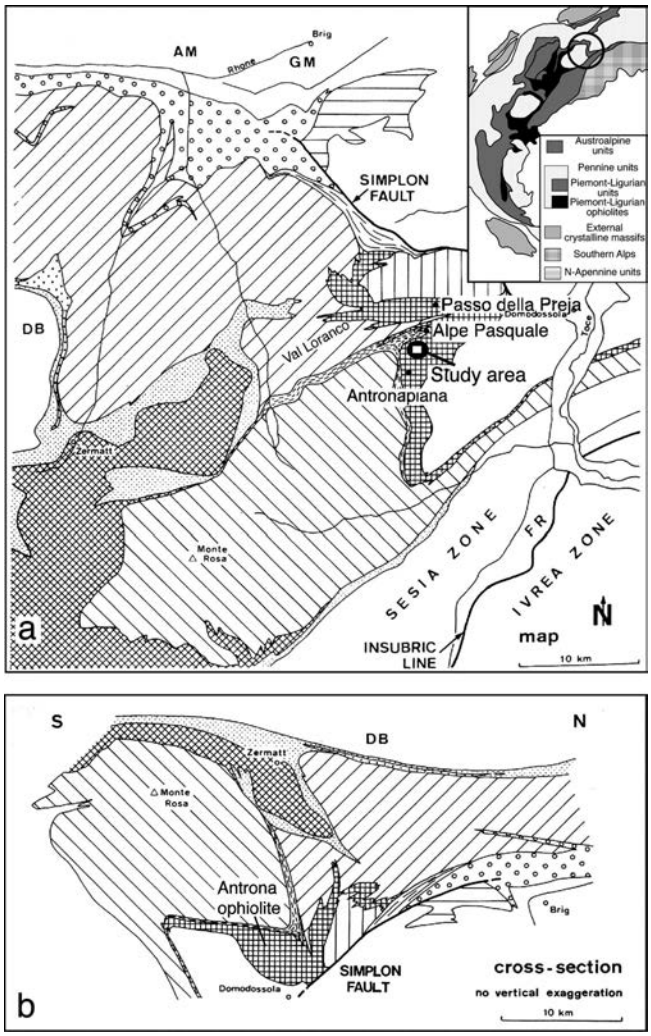

Fig. 1 - Tectonic map (a) and cross-section (b) of the Pennine Alps in the western Central Alps (modified after Milnes et al., 1981). The inset shows the location of the study area in the central-western portion of the Alpine chain.

ble of pre-Mesozoic (?) age (Bearth, 1954). In the upper part, it includes layers (tectonic transposition) of Mesozoic metasediments (tabular quartzites, dolostone, carnieule, calcschists) and tectonically transposed ophiolite rocks of the underlying Antrona Unit (Blumenthal, 1953; Bearth, 1957; 1964; Dal Piaz, 1966; Wetzel, 1972;). According to Dal Piaz (Dal Piaz, 1964; 1966), the Furgg Zone exposed in the southern Monte Rosa has a pre-granitic protolith, free of Mesozoic rocks and was affected by eclogitic to greenschists facies Alpine metamorphism. More recently, the Furgg Zone has been interpreted as cover portions of the Monte Rosa basement (Jaboyedoff et al., 1996; Escher et al., 1997; Steck et al., 2001) or of the continental Portjengrat Unit (Keller and Schmid, 2001). Alternatively, the Furgg Zone has been considered as the suture of the Valais basin (Froitzheim, 2001), or a tectonic mélange interposed between the continental Monte Rosa-Portjengrat Units and the Zermatt-Saas and Antrona ophiolites (Kramer, 2000). Based on SHRIMP analyses, Liati et al. (2001) interpreted the Furgg Zone as a tectonic mélange with a strongly heterogeneous composition including Variscan and pre-Variscan basement (510 ± 5 Ma) as well as post Variscan rocks (272 ± 4 Ma), which were affected by Alpine metamorphism (87 ± 20 Ma is the age of metamorphism determined in an amphibolitized eclogite boudin from the Andolla area in the upper Antrona Valley).

The Zermatt-Saas and Antrona metaophiolites, the Monte Rosa Nappe, the Furgg Zone, and the Camughera Moncucco Unit have all experienced regional subduction-related high-pressure metamorphism during the Alpine orogeny. The Zermatt-Saas ophiolite subduction history is attested by the occurrence of lozenge-shaped pesudomorphs of lawsonite and other prograde relics followed by peak eclogitic to UHP mineral assemblages (Ernst and Dal Piaz, 1978; Oberhänsli, 1980; Barnicoat and Fry, 1986; Martin and Tartarotti, 1989; Reinecke, 1991; 1998). Eclogite rocks in the Antrona ophiolite have been described by Colombi and Pfeifer (1986). In the Monte Rosa Nappe, the Alpine eclogitic imprint has been recognized in both the pre-granitic complex (Dal Piaz and Lombardo, 1986; Borghi et al., 1996; Michard et al., 1996; Keller et al., 2005a) and in the orthogneisses (Dal Piaz and Gatto, 1963; Dal Piaz and Lombardo, 1986). More recently, eclogite mineral assemblages have been recognized also in the Camughera-Moncucco Nappe (Keller et al., 2005b).

During decompression accompanying exhumation, the Zermatt-Saas and upper Monte Rosa Units were re-equilibrated under greenschist facies conditions (Frey et al., 1974; Ernst and Dal Piaz, 1978; Keller et al., 2005a). The lower parts of Monte Rosa and the Antrona ophiolite underwent epidote-amphibolite facies metamorphism (Pfeiffer et al., 1989).

The Antrona Nappe

The Antrona Nappe is exposed in the Antrona-Loranco-Anzasca Valleys, on the Italian side, and in the Laggintal - Simplon area, on the Swiss side (Fig. 1). In Italy, the Antrona ophiolites are also exposed in the Bognanco Valley (north-east of Antrona) and can be followed to the Vigezzo Valley east of Domodossola. In the lower Bognanco Valley, rocks interpreted as belonging to the Antrona ophiolite define the contact between the Camughera-Moncucco and Monte Leone Nappe (Keller et al., 2005b). The main lithologies in the Antrona area (Antrona and Anzasca Valleys) were described by Laduron and Merlin (1974), Laduron (1976), Colombi and Pfeifer (1986), Colombi (1989), Pfeifer et al. (1989). The typical Antrona ophiolite suite includes serpentinized ultramafites, metagabbros and metabasic rocks. In the nearby Bognanco Valley, Carrupt and Schlup (1998) described a detailed ophiolitic section consisting of N-MORB to T-MORB-type metabasalts and minor serpentinite and gabbros. This ophiolite is covered by (from bottom to top) garnet-micaschists, metaquartzites, calcschists and intercalated metabasite, sedimentary breccia, pure calcschists, marbles, and graphitic marbles. The Antrona ophiolite is dominated by a Tertiary amphibolite facies metamorphism. Mafic eclogites containing garnet, symplectites, amphibole and relict omphacitic clinopyroxene have been described by Colombi and Pfeifer (1986) in the Antrona-Anzasca area. Minimum pressures of 14-16 kbars at 480-720 °C were suggested for the high pressure stage of these rocks by these authors.

FIELD RELATIONSHIPS OF OPHIOLITE ROCKS IN THE ANTRONA VALLEY

The study area is located in the upper Antrona Valley, between Alpe Pasquale, to the north, and the village of Antronapiana, to the south (Fig. 1); it was mapped in detail

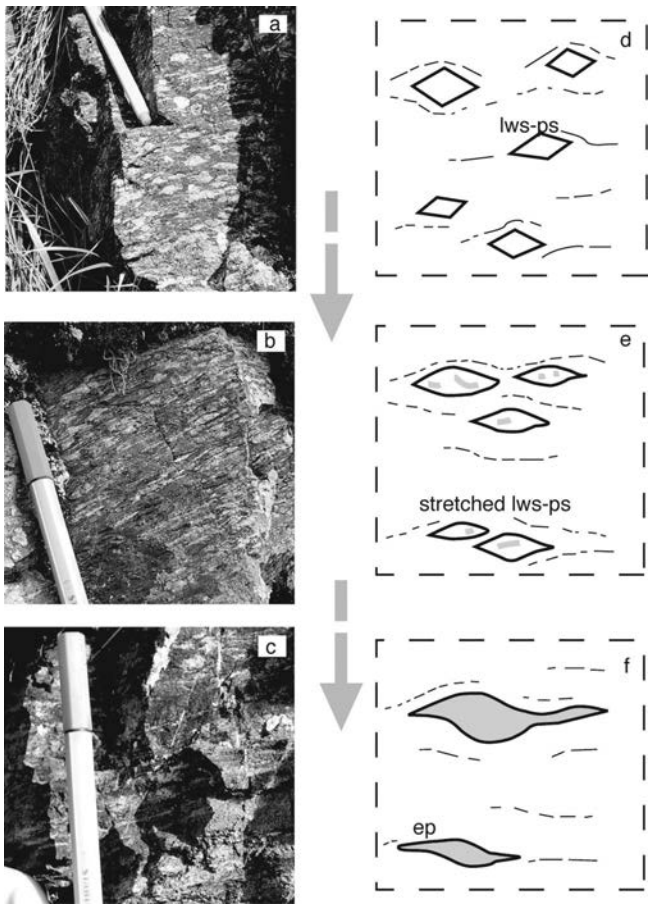

Fig. 2 - Photographs of lawsonite (pseudomorphed)-bearing amphibolites (a, b) and epidote-amphibolite (c). d-e-f) Cartoons showing the microstructural evolution and mineral changes from lawsonite-bearing amphibolite to epidote-amphibolite. a, d) Lozenge-shaped pseudomorphs (lws-ps) consisting of epidote, chlorite, and carbonate. b, e) Pseudomorphs are deformed by stretching. c, f) Stretched pseudomorphs evolve to mm-thick layers, mostly consisting of epidote.

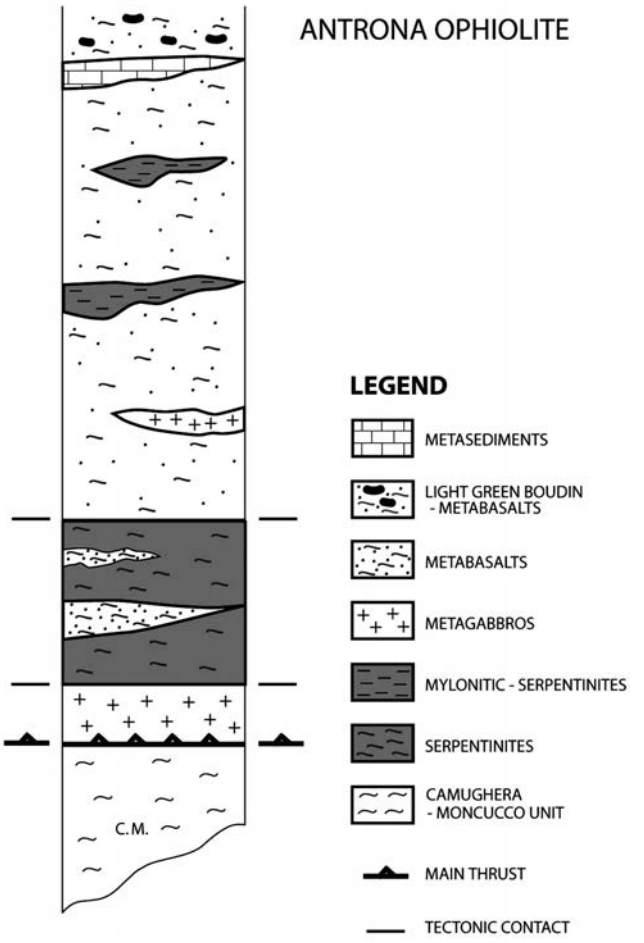

Fig. 3 - Simplified lithostratigraphic column of the ophiolite suite in the Antrona valley.

at the scale of 1: 5000 by Turco (2004). In this area, metamorphosed ophiolites are exposed along the eastern side of the Antrona Valley. The main rock types are ultrabasic rocks, metagabbros and metabasalts. Ultrabasic rocks are mostly serpentinized and make up a 35 km^2 body extended from Antronapiana to Pizzo Ciapé, near the tectonic contact with the Camughera-Moncucco Unit. Serpentinite structures range from massive to mylonitic. Mylonitic serpentinites are interlayered within metabasites. Dark green fine-grained amphibolite dikes are interlayered within massive serpentinites near Antronapiana. The contact between serpentinites and metabasalts at the northern border of the massif is commonly marked by actinolite-schists. To the south of Antronapiana, serpentinites are in tectonic contact with Mg-metagabbros. This contact does not show any reaction zone. Outcrops of metagabbros are rare and restricted to m-scale layers associated with metabasalts. A body of Mg-metagabbro up to 50 m in thickness crops out at Pizzo Ciapé, near the divide with the Bognanco Valley. Metagabbro has transitional contacts with prasinite and their macroscopic distinction is usually based on structure and grain size .

Metabasites are the most abundant rock type in the studied ophiolite suite. These rocks are characterized by fine grain-size and dark blackish-green colours. On the basis of mineral components and structure, we differentiated the following types: amphibole-eclogites, garnet-amphibolites, lawsonite (pseudomorphosed)-bearing amphibolites, epidote- amphibolite, pale green microboudin-bearing amphibolites. Amphibole-eclogites are very scarce (one main m-scale layer near the Fornalino Pass). The high-pressure mineral assemblage consists of garnet-Na-clinopyroxene-rutile and amphibole ± quartz.

Amphibolites are the dominant rock type in the working area. Garnet-rich amphibolites are fine-grained dark green rocks characterized by the strong mineral lineation of amphibole crystals. Lawsonite (pseudomorphosed)-bearing amphibolites (see next section) are macroscopically recognizable for the occurrence of whitish, centimetric lozenge-shaped crystals (Fig. 2). So far, lawsonite (now pseudomorphosed)-bearing rocks have not been documented in the study area. Epidote-amphibolites are typically characterized by the presence of millimetric yellow-green epidote-rich layers alternating with dark green amphibole-rich layers. One rock type commonly grades into the other (Figs. 2a, 2c). The structural evolution from one type to the other is marked by increasing stretching of the cm-sized and lozenge-shaped pseudomorphs on lawsonite, followed by crystallization of epidote in planar, mm-thick layers (Figs. 2d, 2f). A further rock type recognized in the field (best outcrops along the right side of the Alpe Cavalli Lake in the

Table 1 - Lithologies and petrographic features of the studied metaophiolite in the Antrona valley.

Rock	Micro-structure	Eo-Alpine mineralogy	Meso- and Neo-Alpine mineralogy
Metagabbro	Flaser to mylonitic	(Na-clinopyroxene? zoisite?), amphibole	Amphibole, chlorite, clinozoisite, pistacite
Amphibole Eclogite	Massive polygonal to interlobate	Garnet, Na-clinopyroxene, amphibole core, rutile	Amphibole rim, amph-plag symplectites, titanite
Garnet amphibolite	Nematoblastic-porphyroblastic	Garnet, amphibole, feldspar, quartz	Chlorite, clinozoisite, amphibole
Lawsonite -bearing amphibolite	Nematoblastic	(Laws), amphibole, garnet, rutile	Amphibole, chlorite, biotite, plag, epidote, titanite
Epidote amphibolite	Nematoblastic	Amphibole, (laws?, garnet?),	Pistacite, chlorite, amphibole
Microboudin-bearing amphibolite	Nematoblastic- symplectitic?	Amphibole, garnet, (Na-clinopyroxene?), rutile	Amphibole-plag symplectite, amphibole around garnet, clinozoisite
Prasinite	Granoblastic to schistose	no relics	Amphibole (Actinolite), plag, chlorite, epidote, quartz
Serpentinite	Porphyroclastic to schistose to mylonitic	Olivine, serpentine, spinel	Serpentine, magnetite
Quartzite	Granoblastic to schistose	Quartz, white mica, garnet	Quartz, white mica, brown biotite
Micaschist	Schistose-porphyroblastic	White mica, garnet, chloritoid, quartz	White mica, brown biotite, chlorite
Marble	Granoblastic	Carbonate, quartz, biotite, white mica	Chlorite, epidote
Calcschist	Schistose-granoblastic	Carbonate, quartz, white mica,	Clinozoisite, biotite

Loranco Valley) is characterized by the occurrence of dm-scale boudins of pale green amphibolite inside dark green amphibolite. Lawsonite pseudomorphs, epidote-rich layers and boudins within amphibolites show a preferential orientation parallel to the regional main schistosity.

Metasediments of the ophiolite suite in the Antrona Valley are mostly represented by garnet-quartzites, micaschists, marbles and calcschists.

A representative lithostratigraphic column of the ophiolite suite mapped in the Antrona Valley is shown in figure 3.

PETROGRAPHY

Rock types and microstructural features of the investigated samples are summarized in Table 1. In the studied rocks four main foliations were recognized, related to ductile deformation phases D1-D4. S1 is the oldest foliation, locally preserved inside garnet; S2 corresponds to the regional foliation seen in the field, and is mostly marked by amphibole and garnet; S3 and S4 are younger foliations cutting S2, and are commonly defined as crenulation cleavage or S-C struc-

tures marked by chlorite and albite. All ductile structures are cut by veins filled with prehnite-pumpellyite facies minerals. Four stages of mineral crystallization (B1-B4) were recognized in the studied mafic rocks (see Fig. 9 and Discussion).

Ultrabasic rocks

Ultrabasic rocks consist largely of serpentine (antigorite), magnetite, and minor diopside and talc. Olivine can be found in more massive rock types, where it is present in coarser-grained (mm) stretched grains (olvine I) and fine-grained neoblast (olivine II). This texture suggests that olivine I underwent grain-size reduction by recrystallization during the Alpine deformation (Fig. 4a). Coarse-grained olivine exhibits undulatory extinction and subgrains. The shape of subgrains reminds the microstructure of porphyroclastic olivine in mantle peridotites (Mercier and Nicolas, 1975; Nicolas and Poirier, 1976). Amphibolite dikes interlayered with massive olivine-bearing serpentinites consist of amphibole (85-90%), plagioclase (5-10%), titanite (5%), epidote (1%). They exhibit a fine-grained granoblastic texture.

Metagabbro

Metagabbro samples consist of amphibole (50-60%), epidote (15-30%), plagioclase (10-20%), quartz (5-10%), chlorite (2-10%), opaque (1%), ± biotite, carbonate. Their microstructure varies from weakly schistose with relics of magmatic microstructures, to flaser and mylonitic. In flaser metagabbro, the foliation (S2) is spaced and defined by amphibole films alternating with lithons made of epidote and plagioclase (Fig. 4b). Amphibole, epidote and plagioclase crystallization pertains to B3 stage. Foliation wraps around mm-sized, sigmoidal or stretched porphyroclasts of former clinopyroxene now replaced by coarse-grained amphibole grains. Strain shadows are commonly filled with fine-grained amphibole, quartz, ± epidote, chlorite (stages B3, B4).

Amphibole-eclogite

This rock consists of medium-grained, inequigranular garnet (35-40%), amphibole (20-45%), Na-clinopyroxene (10-20%), amphibole + plagioclase symplectites (2-10%), ± quartz, rutile (Fig. 4c). Microstructure ranges from polygonal to interlobate. Garnet is present in subhedral to euhedral

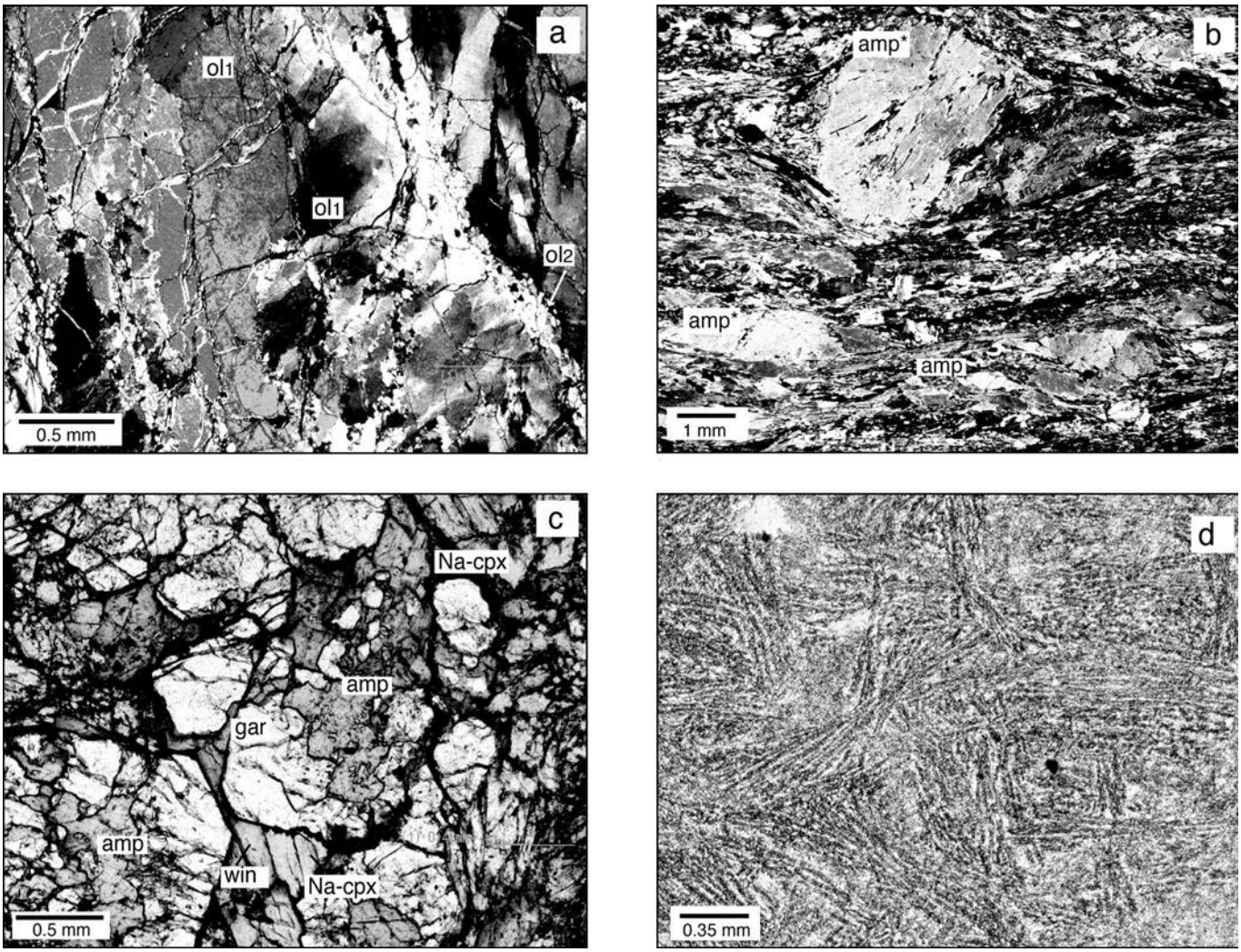

Fig. 4 - Photomicrographs of selected ophiolite samples from the Antrona valley. a) Ultrabasic rock: coarse-grained (ol1) and fine-grained neoblasts (ol2) of olivine, cut by veinlets filled with antigorite (left side of the picture). Crossed polars. b) Flaser metagabbro: porphyroclasts of former clinopyroxene now replaced by coarse-grained amphibole grains (amp*). Strain shadows are filled with fine-grained amphibole, quartz, ± epidote, chlorite. Crossed polars. c) Amphibole-bearing eclogite: garnet (gar), partially replaced by subhedral Ca-amphibole (amp), is in contact with both winchite-rich amphibole (win) and Na-clinopyroxene (Na-cpx). Plane polarised light. d) Microboudin-bearing amphibolites: aggregates of acicular crystals with “dendritic”-like or “sheaf”-like structure occurring in a microboudin (see also backscattered picture in Fig. 6b). Plane polarised light.

porphyroblasts or poikiloblasts (scattered inclusions of amphibole). Amphibole occurs either as nematoblasts in textural equilibrium with both garnet and Na-clinopyroxene, or subhedral grains replacing garnet. Amphibole nematoblasts commonly have uncoloured cores and blue-green rims, which correspond to chemical zoning (see next section and Fig. 6b). The core of these amphibole crystals, together with garnet and Na-clinopyroxene, are inferred to pertain to the HP mineral paragenesis (stage B2). Na-clinopyroxene occurs as greenish nematoblasts showing textural equilibrium with garnet and amphibole. The contact between garnet and clinopyroxene is almost always marked by a very thin (µm scale) rim of green amphibole (stage B3) as a reaction product of the two HP mineral phases. Amphibole + plagioclase symplectites were produced by the break-down of Na-clinopyroxene, reacting with quartz to form amphibole + sodic plagioclase through hydration reactions with adjacent minerals during retrogression.

Garnet-amphibolite

The rock consists of amphibole (30-45%), plagioclase (10-25%), epidote (18-20%), carbonate (0-10%), white mica (0-10%), opaque minerals (3-5%), garnet (1-2%), ± quartz, chlorite, titanite. Garnet poikiloblasts are up to 5mm in diameter and include epidote, amphibole, opaque minerals. Garnet may be either partially replaced by green amphibole at the rim of porphyroblasts, or completely overgrown by breakdown products such as amphibole, epidote, plagioclase, and opaque minerals, still retaining the shape of the original mineral. The foliation (S2) of the rock is defined by shape preferred orientation (SPO) of green or blue-green amphibole and epidote (stage B3).

Lawsonite (pseudomorphed)-bearing amphibolite

The rock consists of amphibole (40-60%), epidote (20-30%), plagioclase (15-25%), garnet, chlorite (5%), carbonate (0-5%), rutile-titanite (1%), ± opaque, biotite, quartz. The main foliation (S2) is defined by amphibole SPO (stage B3). Millimetric lozenge-shaped porphyroblasts made up of epidote (clinozoisite and pistacite) + chlorite, titanite ± carbonate aggregates were identified (stages B3-B4). The shape of these porphyroblasts range from lozenge to sig-

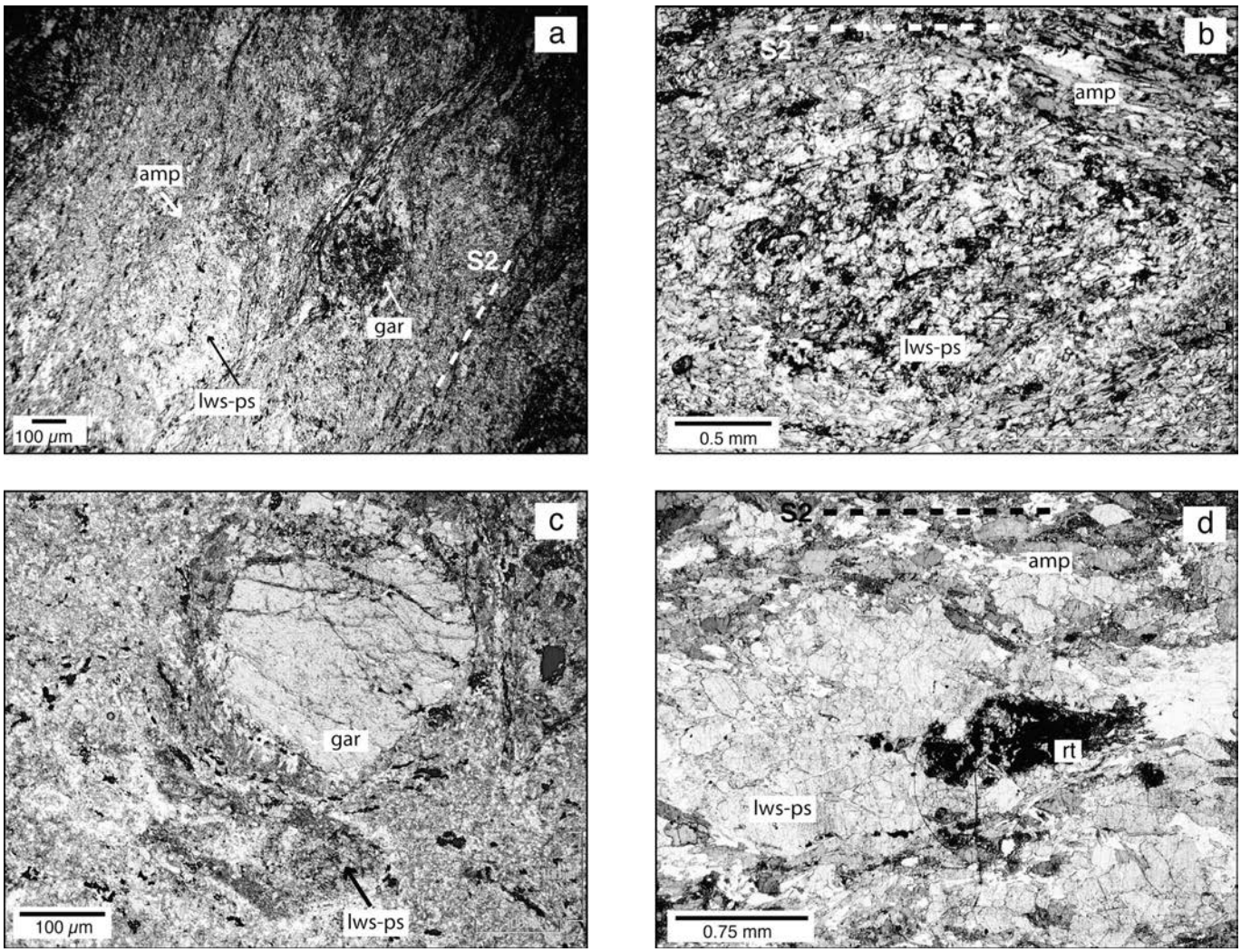

Fig. 5 - Photomicrographs of lawsonite (pseudomorphed)-bearing amphibolite. a) General view of the rock showing millimetric lozenge-shaped to sigmoidal porphyroblasts inferred to replace former lawsonite (lws-ps) and garnet porphyroblast (gar) partially replaced by amphibole. Foliation (S2) defined by amphibole (amp) wraps around porphyroblasts. Plane polarised light. b) Detail of a lozenge-shaped porphyroblast consisting of epidote + chlorite, titanite ± carbonate. Minerals exhibit a slight preferential orientation oblique to the matrix foliation (S2). Plane polarised light. c) Lozenge-shaped porphyroblasts (lws-ps) occurring together with fresh or partially altered garnet in the same sample. Plane polarised light. d) Lozenge-shaped porphyroblasts (lws-ps) consisting of pistacite are boudinaged and include a sigmoidal aggregate of rutile (rt) near the neck between boudins. Plane polarised light.

moidal, according to the intensity of shearing affecting the rock (Figs. 5a, 5b). In general, the porphyroblasts show a preferential shape orientation; their forming minerals exhibit a slight preferential orientation almost oblique to the matrix foliation (Fig. 5b). Lozenge-shaped porphyroblasts may occur together with fresh or partially altered garnet in the same sample (stage B2?; Fig. 5c). In some samples the lozenge-shaped aggregates are deformed by boudinage or are stretched to form mm-thick layers parallel to the foliation. In one sample, microboudins consisting of pistacite include a sigmoidal aggregate of rutile near the neck of boudins (Fig. 5d). This texture suggests that lawsonite and rutile coexisted before or during boudinage affecting the foliation (S2) defined by epidote + amphibole.

In all samples, the matrix foliation wraps around the lozenge-shaped porphyroblasts, as well as garnet porphyroblasts (see Figs. 5a) indicating that both porphyroblasts growth took place before or during the ductile deformation generating the foliation. Based on the shape of porphyroblasts and on their forming minerals, we interpret the porphyroblasts as pseudomorphs after former lawsonite. Epidote + chlorite represent the main products of lawsonite breakdown.

Epidote amphibolite

The common mineral assemblage includes epidote (40-60%), amphibole (20%) plagioclase (5-15%), carbonate (0-10%), chlorite (5-20%), brown biotite (5-10%), opaque minerals (1-12%), titanite (1-2%), and quartz (1-2%). Foliation (S2) is defined by compositional layering marked by mm- to cm epidote-rich layers alternating with amphibole-rich layers, and by SPO of epidote and amphibole crystals (stage B3). In one sample, S2 foliation marked by green amphibole is cut by mm-scale veins filled with prehnite (later than B4).

Microboudin-bearing amphibolites

The host rock consists of amphibole (35-50%), microcrystalline plagioclase + amphibole symplectites (20-30%), plagioclase (15-29%), epidote s.l. (20-25%, carbonate (0-5%, opaque minerals (ca. 1%) ± garnet, white mica, rutile. Microstructure is characterized by mm- to cm compositional layering of symplectites (undetermined under the microscope) alternating with layers of amphibole + epidote + plagioclase. Boudins (cm-scale) have a microcrystalline symplectitic structure, similar to that of symplectite layers in the host rock. Some portions of symplectites in the boudin consist of aggregates of acicular crystals arranged in a “dendritic”-like or “sheaf”-like structure (see Fig. 4d; see also backscattered picture in Fig. 6a). It is inferred that microcrystalline symplectites (stage B3) correspond to the breakdown of former Na-clinopyroxene, whilst aggregates with “sheaf”-like structure are due to recrystallization of symplectites (B4?). Petrographic and microstructural analysis suggest that the microboudin-bearing amphibolites represent transposed micropillow or pillow-breccia basalts.

MINERAL CHEMISTRY AND THERMOBAROMETRY

Analytical methods

Mineral analyses of selected samples of the Antrona ophiolite rocks were performed at CNR-IPDA in Milano by using a SEM Cambridge System Stereoscan 360, equipped with an Energy Dispersive Spectrometer (EDS). The correction program is ZAF4 (Pouchou and Pichoir, 1985). Operating conditions were: accelerating voltage = 20kV, working distance = 25 mm, probe beam = 400 picoampere, count time = 50s. Selected SEM-EDS analyses are reported in Table 2.

Only eclogite samples were analysed also at CNR-IGG in Padova with a Cameca SX50 electron microprobe, equipped with four WDS spectrometers. Operating conditions: 15 KeV acceleration voltage and 15 nA sample current; count time = 10 sec at peak, 5 sec at background. The correction program is PAP (Kato, 2005). Natural and synthetic standards were used.

SEM-EDS analyses

SEM-EDS technique is particularly useful for revealing detailed microstructures, such as symplectites or intergrowths, chemical heterogeneity, etc., providing at the same time (although semi-quantitative) chemical compositions of the observed mineral phases (e.g., Vernon, 2004 and refs. therein). In this study, SEM-EDS was utilized for analyzing the chemical heterogeneity in eclogite amphibole and the fine-grained “symplectites” in the pale green microboudins occurring in amphibolites (see photomicrographs in Figs. 4c and 4d, respectively).

Backscattered images revealed chemical heterogeneities of amphiboles in eclogite (Fig. 6a). SEM chemical compositions of amphibole in eclogites are plotted in Fig. 7; selected analyses are reported in Table 2. Amphibole in the eclogite groundmass is zoned with a core of winchite and rim of Mg-katophorite, taramite, and Fe-tschermakite (Figs. 7d, 7c and 7b, respectively). Amphibole coronas in contact with garnet range from barroisite to Fe-pargasite and Fe-tschermakite (Figs. 7d, 7a). In eclogites, amphibole is also included in garnet; its composition ranges from actinolite and Fe-pargasite to barroisite (Figs. 7a, 7b, 7d).

Backscattered images show that microboudins in amphibolites are characterized by granoblastic structure (Fig. 6b). Mineral phases constituting this fine-grained rock are actinolite, clinozoisite-pistacite, and albite (Table 2).

Representative compositions of amphibole crystals from amphibolites and metagabbro are plotted in Fig. 8. A selection of these analyses is reported in Table 2. Most amphiboles are Ca-amphiboles, ranging in composition from actinolite to Mg-hornblende (Figs. 8a, 8d), and from edenite to Fe-pargasite (Fig. 8b). Barroisitic amphibole was found in almost all amphibolite samples (Fig. 8c).

Plagioclase of all the analyzed amphibolites and metagabbro shows a wide composition ranging from Ab = 70-99%, An = 1-30%.

Microprobe analyses of eclogite minerals

Mineral compositions of amphibole, clinopyroxene, and garnet from amphibole-eclogites are reported in Tables 3 and 4. These quantitative analyses were used for thermometry calculation (see next paragraph).

Amphibole in the groundmass of eclogite samples is not homogeneous. Chemical zoning from core to rim revealed by backscattered images (see Fig. 6a) and SEM-EDS analyses seems to be not confirmed by electron microprobe analyses that provide either actinolite or winchite compos-

Table 2 - Selected SEM-EDS analyses from eclogite samples of the Antrona ophiolite.

AMPHIBOLE

Lithology	Eclogite	Eclogite	Eclogite	Eclogite	Eclogite	Eclogite	Anf bd	Met gb	Met gb	Anf lw	Anf gr	Anf ep
Sample	C1	C1	C14B	C1	C1	C1	C30	C49	C49	C52	C25	C26
Analysis	113	114	144	107	111	112	27	5	9	68	22	138
Occurrence	core	rim	cn	cn	incl	incl	sym			cn		
SiO2 wt%	54.90	48.46	50.45	38.92	54.99	51.11	53.73	55.51	53.21	39.95	50.5	48.07
TiO2	0.14	0.09	0.16	0.02	0.05	0.16	0.01	0.01	0.1	0.57	0,00	0.29
Al2O3	3.27	9.25	8.32	17.52	1.79	7.94	2.1	2.2	5.59	17.66	8.31	7.59
MnO	0.15	0.15	0.22	0.2	0,00	0.1	0.03	0.1	0.1	0.16	0.3	0.34
FeO	12.5	16.50	14.88	20.9	12,00	15.7	9.3	6.92	7.38	16.78	12.49	13.36
MgO	14.74	10.23	11.4	5.05	16.83	12.47	17.18	19.71	17.59	7.64	13.2	13.59
CaO	8.58	8.72	7.98	9.7	10.08	6.66	12.97	11.98	11.47	11.53	7.97	11.98
Na2O	3.57	4.18	2.81	4.56	2.39	4.99	1.13	1.59	1.73	3.06	3.65	1.04
K2O	0.03	0.07	0.08	0,00	0.22	0,00	0,00	0.07	0,00	0.4	0.16	0.15
Total	97.88	97.65	96.30	96.87	98.35	99.13	96.45	98.09	97.17	97.75	96.59	96.41
Si	7.807	7.110	7.287	5.969	7.748	7.192	7.793	7.729	7.490	5.986	7.240	7.025
Al(IV)	0.193	0.890	0.713	2.031	0.252	0.808	0.207	0.271	0.510	2.014	0.760	0.975
sumT	8.000	8.000	8.000	8.000	8.000	8.000	8.000	8.000	8.000	8.000	8.000	8.000
Al(VI)	0.355	0.709	0.703	1.136	0.045	0.508	0.152	0.090	0.417	1.105	0.645	0.332
Ti(VI)	0.015	0.010	0.017	0.003	0.005	0.017	0.001	0.001	0.011	0.064	0.000	0.032
Fe3+	0.203	0.215	0.702	0.346	0.458	0.896	0.000	0.164	0.141	0.112	0.622	0.503
Mg	3.125	2.237	2.455	1.155	3.536	2.616	3.715	4.091	3.691	1.707	2.822	2.961
Fe2+	1.284	1.810	1.096	2.335	0.956	0.951	1.128	0.642	0.728	1.991	0.875	1.130
Mn	0.018	0.019	0.027	0.025	0.000	0.012	0.003	0.012	0.012	0.021	0.036	0.042
sumC	5.000	5.000	5.000	5.000	5.000	5.000	4.999	5.000	5.000	5.000	5.000	5.000
Ca	1.307	1.371	1.235	1.594	1.521	1.004	2.000	1.787	1.730	1.851	1.224	1.876
Na	0.693	0.629	0.765	0.405	0.479	0.996	0.000	0.213	0.270	0.149	0.776	0.124
sumB	2.000	2.000	2.000	2.000	2.000	2.000	2.000	2.000	2.000	2.000	2.000	2.000
Na	0.291	0.560	0.022	0.951	0.174	0.365	0.318	0.216	0.202	0.740	0.239	0.171
K	0.005	0.013	0.015	0.000	0.040	0.000	0.000	0.013	0.000	0.077	0.029	0.028
sumA	0.296	0.573	0.037	0.951	0.214	0.365	0.334	0.229	0.202	0.817	0.268	0.199
catsum	15.296	15.573	15.037	15.951	15.214	15.365	15.333	15.229	15.202	15.817	15.268	15.199
	Win	Mgkat	Bar	Al-Feparg	Act	Febar	Act	Act	Mghor	Al-Feparg	Bar	Mghor

EPIDOTE

Lithology	Amph bd	Amph bd	Amph ep	Amph ep
Sample	C39	C39	C45AA	C45AA
Analysis	135	138	27	28
Occurrence			core	rim
SiO2 wt%	38.79	38.26	37.60	38.37
TiO2	0.00	0.18	0.11	0.13
Al2O3	29.45	28.32	23.48	28.56
Cr2O3	0.00	0.00	0.00	0.00
Fe2O3	5.32	6.55	13.20	7.07
MnO	0.03	0.00	0.14	0.00
MgO	0.05	0.21	0.13	0.26
CaO	24.27	23.78	23.11	23.98
Total	97.91	97.30	97.77	98.37
Si	5.996	5.977	5.993	5.940
Ti	0.000	0.022	0.013	0.015
Al	5.365	5.213	4.411	5.212
Cr	0.000	0.000	0.000	0.000
Fe3	0.619	0.770	1.583	0.824
Mn	0.003	0.000	0.020	0.000
Mg	0.011	0.050	0.030	0.059
Ca	4.019	3.980	3.947	3.977
Total	15.380	15.170	15.934	15.129

PLAGIOCLASE

Lithology	Amph bd	Amph bd	Amph lw	Amph ep	Met gb
Sample	C30	C30	C54	C45AA	C55B
Analysis	49	60	229	36	92*
SiO2 wt%	60.48	67.86	63.56	62.61	60.05
TiO2	0.00	0.00	0.06	0.09	0.08
Al2O3	24.8	19.11	23.87	22.41	24.55
FeO	0.28	0.04	0,00	0.25	0.02
MnO	0.00	0.13	0.06	0.00	0.09
MgO	0.17	0.01	0.00	0.00	0.19
CaO	6.32	0.06	4.6	3.84	6.29
Na2O	8.76	12.58	8.6	10.28	8.94
K2O	0.07	0.03	0.05	0.10	0.03
Total	100.87	99.82	100.79	99.57	100.23
Si	2.679	2.984	2.782	2.793	2.678
Ti	0.000	0.000	0.002	0.003	0.003
Al	1.295	0.990	1.231	1.178	1.290
Fe2	0.010	0.001	0.000	0.009	0.001
Mn	0.000	0.005	0.002	0.000	0.003
Mg	0.011	0.001	0.000	0.000	0.012
Ca	0.300	0.003	0.216	0.183	0.300
Na	0.752	1.072	0.730	0.889	0.772
K	0.004	0.002	0.003	0.006	0.002
Total	5.051	5.058	4.966	5.062	5.062
Anorthite	27.84	0.24	22.70	16.86	27.53
Albite	69.82	98.94	76.78	81.76	70.79
Orthoclas	0.35	0.14	0.31	0.52	0.18

Amph bd: microboudin in amphibolite; amph lw: amphibolite with pseudomorphs after lawsonite; amph ep: epidote amphibolite; met gb; metagabbro. Amphibole structural formula recalculated using the method of Richard and Clark (1990), based on 23 oxygens. Total number of cations = 15 excluding K. Nomenclature after Leake et al. (1997). Unit formula of epidote based on 25 oxygens, and of feldspar on 8 oxygens.

Table 3 - Selected electron microprobe analyses of amphibole and clinopyroxene from eclogite samples of the Antrona ophiolite.

	AMPHIBOLE						CLINOPYROXENE				
SAMPLE	C1	C1	C1	C1	C1	SAMPLE	C1	C1	C1	C1	C14
Analysis	C1AN3	C1CAN1	C1CAN2	C1CAN3A	C1CAN4	Analysis	C1APX2*	C1APX4*	C1EPX1*	C1EPX2*	C14BPX1
Occurrence	incl. in gar	rim/gar	core	core	rim/gar	Occurrence	rim	core	rim	rim	rim
SiO2 wt%	57.61	56.12	56.22	54.57	54.34	SiO2 wt%	55.05	54.82	54.76	54.71	56.26
TiO2	0.01	0.01	0.01	0.00	0.00	TiO2	0.03	0.03	0.02	0.06	0.07
Al2O3	7.81	3.26	2.71	4.85	3.81	Al2O3	4.53	2.98	3.96	4.18	7.20
Cr2O3	0.00	0.00	0.01	0.00	0.00	Cr2O3	0.00	0.03	0.00	0.06	0.00
FeOt	14.72	11.64	12.61	13.20	14.07	FeOt	10.18	10.74	10.94	10.41	6.76
MnO	0.00	0.00	0.01	0.01	0.01	MnO	0.00	0.07	0.02	0.04	0.02
MgO	10.18	15.59	15.97	14.54	14.82	MgO	9.32	10.09	9.54	9.84	9.22
CaO	1.47	8.00	8.64	8.47	8.70	CaO	15.70	16.79	15.27	16.14	14.55
Na2O	6.19	2.60	2.07	2.57	2.23	Na2O	5.67	4.55	5.38	5.05	6.43
K2O	0.00	0.01	0.01	0.00	0.00	K2O	0.00	0.00	0.00	0.00	0.00
Tot	97.99	97.23	98.26	98.21	97.98	Tot	100.48	100.09	99.88	100.48	100.51
Si	8.010	7.900	7.877	7.645	7.665	Si	1.990	2.005	1.998	1.986	2.003
Al	0.000	0.100	0.123	0.355	0.335	Al4	0.010	0.000	0.002	0.014	0.000
SumT	8.010	8.000	8.000	8.000	8.000	tet	2.000	2.005	2.000	2.000	2.003
Al	1.281	0.441	0.325	0.447	0.299	Al6	0.183	0.129	0.169	0.164	0.302
Cr	0.000	0.000	0.001	0.000	0.000	Fe2	0.086	0.137	0.121	0.115	0.063
Fe3	0.367	0.364	0.356	0.606	0.646	Fe3	0.222	0.192	0.212	0.200	0.138
Ti	0.001	0.001	0.001	0.000	0.000	Mg	0.502	0.550	0.519	0.533	0.490
Mg	2.109	3.271	3.335	3.036	3.115	Mn	0.000	0.002	0.000	0.001	0.001
Fe2	1.242	0.923	0.983	0.911	0.940	Ti	0.001	0.001	0.000	0.002	0.002
Mn	0.000	0.000	0.000	0.000	0.000	Cr	0.000	0.001	0.000	0.002	0.000
Ca	0.000	0.000	0.000	0.000	0.000	Oct	0.994	1.011	1.023	1.017	0.995
SumC	5.000	5.000	5.000	5.000	5.000	Xoct	0.000	0.011	0.023	0.017	0.000
Mg	0.000	0.000	0.000	0.000	0.000	Ca	0.608	0.658	0.597	0.628	0.555
Fe2	0.103	0.084	0.139	0.029	0.074	Na	0.398	0.323	0.381	0.355	0.444
Mn	0.000	0.000	0.001	0.001	0.001	M2	1.006	0.991	1.000	1.000	0.998
Ca	0.219	1.207	1.297	1.271	1.315						
Na	1.669	0.710	0.562	0.698	0.610	Jd	18.3	12.9	16.9	15.9	30.0
SumB	1.990	2.000	2.000	2.000	2.000	Ac	22.2	19.2	21.2	19.5	13.8
Ca	0.000	0.000	0.000	0.000	0.000	Wo	30.3	33.2	29.9	31.8	28.1
Na	0.000	0.000	0.000	0.000	0.000	En	25.0	27.8	26	27.0	24.7
K	0.000	0.002	0.002	0.000	0.000	Fs	4.3	6.9	6.1	5.8	3.2
SumA	0.000	0.002	0.002	0.000	0.000						
tot cat	15.000	15.002	15.002	15.000	15.000						
15-K	Glaucophane	Winchite	Actinolite	Winchite	Actinolite						

Amphibole structural formula recalculated using the method of Richard and Clark (1990), based on 23 oxygens. Total number of cations = 15 excluding K. Nomenclature after Leake et al. (1997). Clinopyroxene formula based on 6 oxygens.

tions at the core as well as at the rim of crystals (Table 3). Amphibole inclusions in garnet are glaucophane (Table 3).

Clinopyroxene from eclogite shows compositions ranging from omphacite to aegirine-augite (Table 3), according to Morimoto's (1989) classification.

Garnet in eclogite is characterized by chemical zoning with grossular-rich cores and pyrope-rich rims (Table 4).

P-T conditions of metamorphism

Temperature and pressure conditions of the Alpine metamorphic peak were estimated on amphibole-bearing eclogite samples from the study area. P-T values are constrained by the garnet-Na-clinopyroxene equilibria and the jadeite content in Na-clinopyroxene. Temperature was evaluated as the average of the four more recent calibrations for the garnet-clinopyroxene thermometer (Powell, 1985; Ai, 1994; Krogh, 1998; Ravna, 2000). Six garnet-clinopyroxene pairs were analised and temperatures of T = 372 ± 50°C for a nominal pressure of P = 1 GPa and T = 386 ± 50°C for a nominal pressure of P = 1.5 Gpa were obtained. We found pyroxenes with Jd_{30} as the maximum jadeite content (see Table 3) suggesting P > 1 GPa (Holland, 1983).

DISCUSSION

Rock assemblage and lithostratigraphy

The ophiolite suite exposed in the Antrona Valley consists of serpentinized (mantle) peridotite, metagabbro, metabasalt and metasedimentary cover, largely representing the typical "Penrose"-type ophiolite (Anonymous, 1972). On the basis of field data and petrography, a new recognition of the ophiolite rock types was performed, in order to define the stratigraphy of this portion of oceanic lithosphere. More detailed informations would be obtained by integrating the present results with bulk rock analyses (Tartarotti et al., in prep.). Metabasaltic rocks, defined so

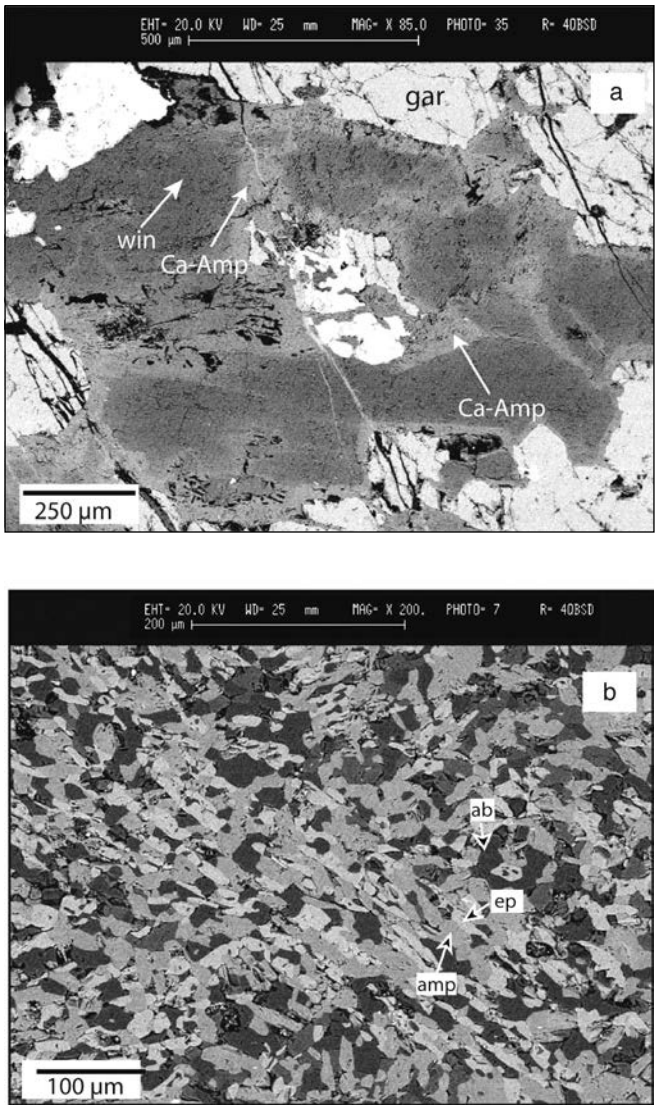

Fig. 6 - BSE images of amphibolite and eclogite samples. a) Chemical zoning in eclogite amphibole: Na-Ca amphibole (win = winchite) corresponds to darker core; lighter Ca-amphibole (Ca-Amp) forms the rims; gar = garnet. b) Detail of the "sheaf"-like structure observed in light green boudins of the microboudin-bearing amphibolites. amp= amphibole; ep = epidote; ab = albite.

far simply as "amphibolites" are tentatively subdivided into different types, on the basis of their mineral composition and microstructural features. New findings are: i) relics of magmatic structures in some amphibolites, inferred to be pillow lavas or pillow breccia; ii) lawsonite pseudomorphs-bearing amphibolites; iii) that epidote-amphibolite of the Antrona Valley derived from lawsonite-bearing amphibolite.

Metamorphic evolution

Petrographic observations and mineral analyses give information about the Alpine tectonometamorphic evolution for the studied ophiolite rocks, summarized in Fig. 9. By integrating microstructural features and structures observed at the meso-scale, at least four Alpine ductile deformation phases (D1-D4) were recognized. These phases produced four metamorphic foliations (S1-S4). Four stages of mineral crystallization (B1-B4) were recognized.

D1 is related to relict microstructures older than D2 (responsible for the main foliation S2). Such microstructures are represented by glaucophane inclusions (B1) inside garnet in the amphibole-eclogite samples. Glaucophane inclusions, however, are scattered and do not define an internal foliation within garnet. Internal foliation marked by rutile and quartz was instead observed inside garnet poikiloblasts in micaceous metaquartzites (Turco, 2004). We infer that glaucophane inclusions and rutile + quartz foliation represent relict of the prograde Alpine metamorphic path likely occurred under blueschist facies conditions. D2 is responsible for the main regional foliation S2 recognizable in the field, mostly defined by Ca-Na- and Ca-amphibole. Before the onset of D2, step B2 (eo-Alpine stage) is responsible for the crystallization of high pressure mineral assemblages including Na-clinopyroxene + winchite + garnet + rutile in mafic rocks (Fig. 9). Step B3 (meso-Alpine stage) produced Ca-Na amphiboles at winchite rims in eclogite and Ca-amphibole + epidote + biotite + plagioclase in amphibolites, marking the S2 foliation. B4 (neo-Alpine stage) is characterized by the growth of actinolite + chlorite + epidote + albite defining the S3 and S4 foliations under greenschist facies conditions. In some samples, chlorite and epidote are not associated with a foliation, when replacing garnet. S3 and S4 foliations are not pervasive and are defined as crenulation cleavage or S-C structures. Finally, B4 was followed by growth of prehnite filling veins cutting through all previous structures.

Microstructural evidence regarding the first appearance of lawsonite in the studied rocks is scarce: relics of (pseudomorphed) lawsonite inside garnet were not observed. Evidence of Na-clinopyroxene-lawsonite coexistence is lacking (Na-clinopyroxene was found in eclogites and not in amphibolites bearing pseudomorphs after lawsonite). Indeed, bulk rock chemistry, in addition to pressure, temperature and volatile components in the system, are among the main factors controlling lawsonite formation (e.g., Pognante, 1989 and refs. therein; Bucher et al., 2005). Such scarce textural evidence prevents a correct definition of the relative chronology of deformation vs. metamorphism. On the basis of textural relations, we infer that the growth of lawsonite porphyroblasts in amphibolites took place before or during D2 which produced S2 foliation defined by (B3) Na-Ca and Ca-amphibole. Consequently, lawsonite (± rutile; see Fig. 5d) is inferred to grow before the onset of the amphibolite or epidote-amphibolite facies conditions.

A qualitative P-T diagram showing the metamorphic evolution the Antrona ophiolite rocks as deduced from the stability conditions of the observed mineral parageneses is illustrated in Fig. 10. The peak P-T condition as estimated in the eclogite samples is also reported (see "B2" in Fig. 10). The prograde event (B1) likely occurred under blueschist facies (as attested by glaucophane inclusions in garnet from eclogite samples) followed by high pressure (eclogitic) metamorphic peak, attested by the omphacite-garnet pair (B2). A possible coexistence of the omphacite-lawsonite pair under eclogite facies conditions cannot be ruled out, if we consider the P-T values obtained by thermobarometric calculation in the eclogite samples. In fact our results ($T = 372 \pm 50$°C for $P \geq 1$ Gpa) are compatible with the stability field of lawsonite (low-T side of the reactions 1 and 2 in Fig. 10). Previous works on eclogites in the studied area suggested that metabasic rocks were equilibrated under P = 1.4 - 1.6 GPa and T = 480-720°C (Colombi and Pfeiffer, 1986). These results have been obtained on garnet - omphacite pairs, follow-

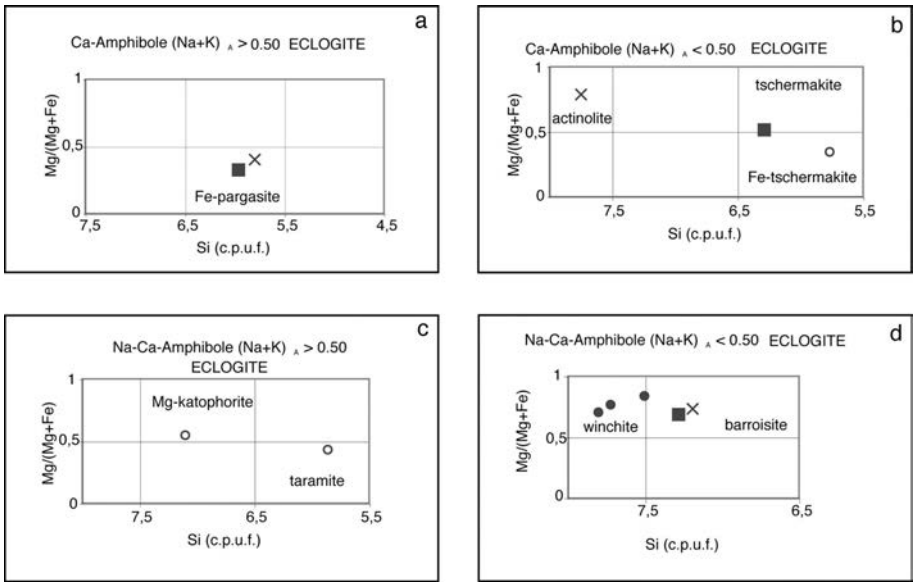

Fig. 7 - Compositions of eclogite amphiboles analysed by SEM-EDS. Nomenclature after Leake et al. (1997). Filled and open circle = core and rim of crystal, respectively; cross = amphibole inclusion in garnet; filled square = amphibole in garnet corona.

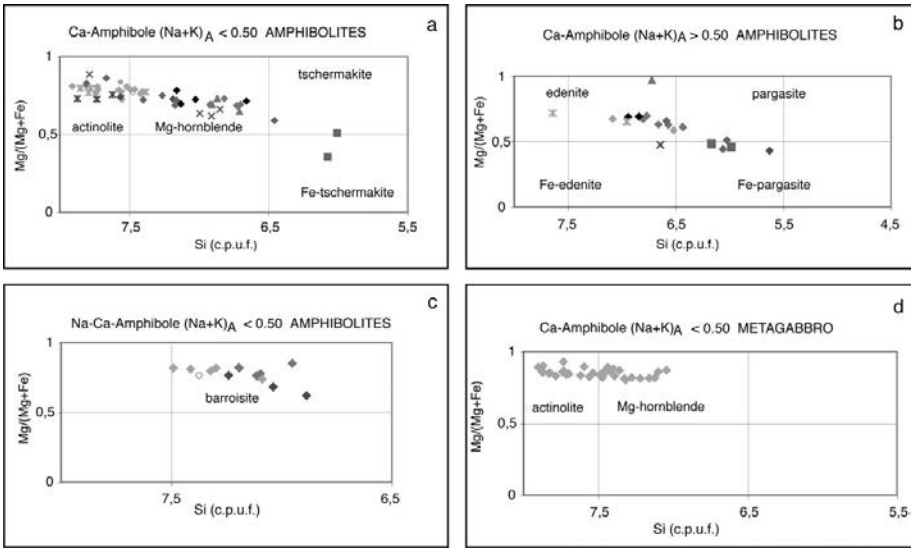

Fig. 8 - SEM-EDS compositions of amphiboles in amphibolites and metagabbro. Nomenclature after Leake et al. (1997). Symbols: cross = amphibole inclusion in garnet; diamond = amphibole on S2 foliation; triangle = amphibole on S3 foliation; filled and open circle = core and rim of crystal, respectively; asterisk = amphibole in symplectite; filled square = amphibole in corona around garnet.

ing the Ellis and Green (1979)'s thermometric calibration. Nevertheless, the suggested temperature span appears to be unreasonably large. In addition, no microchemical analyses or other arguments have been provided by Colombi and Pfeiffer (1986) to explain such a large temperature span. Many analyses (e.g. Lardeaux et al., 1986) suggested that the temperature span obtained with this method may considerably be reduced with a careful textural selection of the analysed sites. Moreover, the Ellis and Green (1979)'s calibration for the garnet-clinopyroxene thermometer probably overstimates temperature (e.g. Green and Adams, 1991) and thus it was not utilised in the present study.

According to Pfeifer et al. (1989), the peak metamorphism of the Antrona metabasic rocks was followed by amphibolite facies conditions, estimated at T = 550°C in metasediments, and then by greenschist facies conditions. According to Carrupt and Schlup (1998), the retrogressive greenschist stage was followed by an increase in temperature, inferred from the compositional zoning of amphibole and plagioclase in mafic rocks. In the present study, the retrograde metamorphic evolution may be inferred from the incipient breakdown of high pressure minerals in the eclogite samples and from the amphibolites samples, that are characterized by epidote-amphibolite/amphibolite facies mineral assemblages (step B3 in Figs. 9 and 10). These mineral assemblages were overprinted by greenschist facies minerals (B4), followed by prehnite-pumpellyite facies mineral assemblages (prehnite-filled veins). Our petrographic observations and mineral chemistry data are consistent with Pfeifer et al. (1989)'s estimates for the retrogressive evolution of the Antrona ophiolite.

CONCLUDING REMARKS AND REGIONAL IMPLICATIONS

Field data and petrographic observations allow a new definition of the ophiolite rock types exposed in the Antrona Valley. New findings are:

- relics of magmatic structures in some amphibolites, inferred to be pillow lavas or pillow breccia;
- lawsonite pseudomorphs-bearing amphibolites;
- the epidote-amphibolites of the Antrona Valley derived from lawsonite-bearing amphibolite;

Table 4 - Selected electron microprobe analyses of garnet from eclogite samples of the Antrona ophiolite.

SAMPLE	C1	C1	C1	C1	C1	C1	C1
Analysis	C1CGT1	C1CGT3	C1CGT4	C1AGT2*	C1AGT3*	C1EGT1*	C1EGT2*
Occurrence	rim	int rim	core	rim	rim	rim/cpx	int rim/cpx
SiO2 wt%	38.56	38.17	37.96	38.39	38.09	38.40	38.08
TiO2	0.09	0.06	0.14	0.07	0.11	0.05	0.09
Al2O3	20.51	20.61	20.46	20.89	20.44	20.43	20.60
Cr2O3	0.00	0.00	0.00	0.04	0.02	0.00	0.00
FeOt	31.74	30.82	28.96	32.12	30.67	31.54	30.86
MnO	1.21	0.23	1.47	0.13	1.28	0.47	0.16
MgO	3.82	2.02	1.47	2.46	1.28	2.73	2.13
CaO	5.95	9.29	11.17	7.87	10.29	7.40	8.83
Na2O	0.00	0.00	0.00	0.01	0.06	0.07	0.00
K2O	0.00	0.00	0.00	0.00	0.00	0.00	0.00
Tot	101.88	101.21	100.43	101.97	101.23	101.10	100.76
Si	3.008	3.007	3.008	3.004	3.008	3.022	3.011
Ti	0.005	0.004	0.008	0.004	0.007	0.003	0.005
Al	1.886	1.914	1.911	1.927	1.902	1.895	1.920
Cr	0.000	0.000	0.000	0.003	0.001	0.000	0.000
Fe3	0.109	0.083	0.081	0.067	0.090	0.102	0.075
Fe2	1.961	1.947	1.839	2.035	1.936	1.974	1.966
Mn	0.080	0.016	0.018	0.009	0.019	0.031	0.011
Mg	0.444	0.238	0.174	0.286	0.151	0.321	0.251
Ca	0.497	0.784	0.949	0.660	0.871	0.624	0.748
Na	0.000	0.000	0.000	0.001	0.009	0.011	0.000
Tot	7.990	7.991	7.987	7.995	7.993	7.982	7.987
Pyrope	14.89	7.96	5.83	9.58	5.06	10.87	8.44
Almandine	65.76	65.25	61.73	68.07	65.05	66.91	66.05
Grossular	11.18	22.12	27.79	18.59	24.67	15.99	21.37
Spessartine	2.68	0.52	0.59	0.29	0.63	1.06	0.36
Andradite	5.48	4.15	4.06	3.34	4.52	5.17	3.77

* utilised for thermobarometric calculations. Structural formula calculated on the basis of 12 oxygens.

- the P-T evolution is characterized by a prograde blueschist-facies stage and by an eclogitic peak occurred at T = 372 ± 50°C and P ≥ 1 GPa. This P-T condition is consistent with the stability of lawsonite, that was observed as pseudomporphs in amphibolites, but not in omphacite-garnet-bearing rocks. The retrograde evolution of the Antrona metabasites occurred under epidote-amphibolite/amphibolite facies overprinted by greenschist facies conditions. Late minerals associated with brittle deformation grew under prehnite-pumpellyite facies conditions.

The inferred metamorphic evolution for the Antrona Unit may be compared, at least in part, to that suggested for the Zermatt-Saas metaophiolite (e.g., Ernst and Dal Piaz, 1978; Barnicoat and Fry, 1986; Fry and Barnicoat, 1987; Bucher et al., 2005): both units exhibit prograde Alpine blueschist mineral assemblages followed by an eclogitic peak, typical for subduction-related metamorphism. However, the P-T condition of the eclogitic peak in the two units are not easily comparable, due to the large span of P-T estimates obtained so far for the Zermatt-Saas eclogites, ranging from 450-780°C and from 1-2.2 GPa (e.g., Ernst and Dal Piaz, 1978; Oberhänsli, 1980; Barnicoat and Fry, 1986; Fry and Barnicoat, 1987; Cartwright and Barnicoat, 2002).

The retrograde path of the Antrona ophiolite differs from those proposed by Barnicoat and Fry (1986) and Fry and Barnicoat (1987) for the Zermatt-Saas Unit. This latter is characterized by an initial rapid cooling to the lawsonite-eclogite field, before the onset of blueschist (glaucophane growth) and then greenschist facies conditions. Although not well contrained in its initial part, decompression path of the Antrona ophiolite is dominated by epidote-amphibolite/amphibolite facies mineral assemblages. Consequently, even if a common prograde path may be envisaged for the Zermatt-Saas and Antrona ophiolite, their respective exhumation histories probably became different, accounting for their different tectonic positions in the Alpine nappe pile.

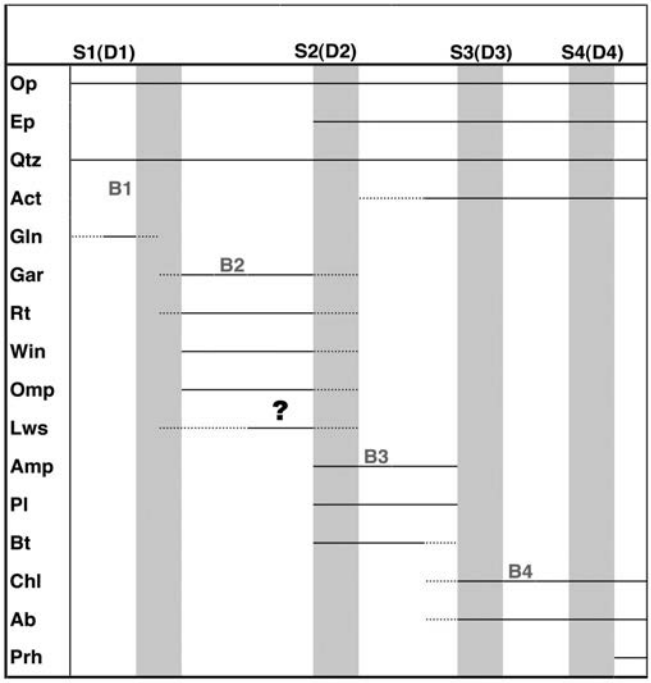

Fig. 9 - Deformation (D) and foliation (S) vs. mineral growth (B) inferred for the studied ophiolite samples from the Antrona ophiolite. Mineral abbreviations according to Kretz (1983).

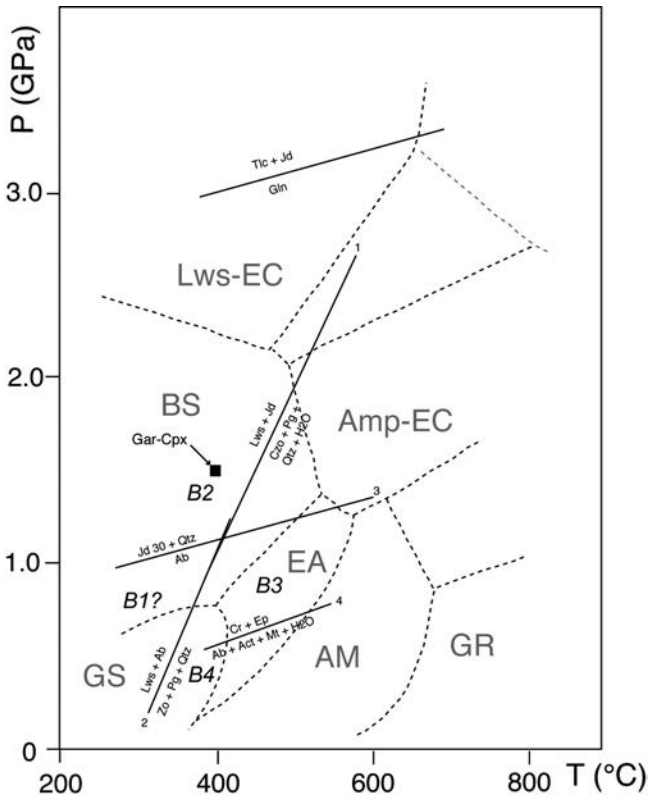

Fig. 10 - Petrogenetic grid with critical reactions defining the metamorphic evolution of the Antrona ophiolite rocks. B1 – B4 represent stages of mineral crystallization as defined in figure 9. Black square indicates the P-T conditions estimated as the average of four gar-cpx thermometers (Powell, 1985; Ai, 1994; Krogh, 1998, and Ravna, 2000), and by considering the maximum jadeite content in clinopyroxene (Holland, 1983). Metamorphic facies fields after Spear (1993). Reaction curves: 1) lws+jd = zo+pg+qtz+H2O (Heinrich and Althaus, 1980); 2) lws+ab = zo+pg+qtz+H2O (Heinrich and Althaus, 1980); 3) omp (jd30) + qtz = ab (Holland, 1983) 4) crossite+ep = ab+act+mag+H2O (Maruyama et al., 1986). Mineral abbreviations according to Kretz (1983).

AKNOWLEDGMENTS

Thanks are due to Piera Spadea and Alessandra Montanini, editors of this Volume, for encouraging the publication of this paper. Critical revisions by Bruno Lombardo, Lukas Keller, and an anonymous referee greatly improved the manuscript. Luca Benciolini is thanked for the critical reading of the manuscript.

P.T. aknowledges research grants FIRST 2005 from Prof. G. Gosso.

REFERENCES

Ai Y., 1994. A revision of the garnet-clinopyroxene Fe^{2+}-Mg exchange thermometer. Contrib. Mineral. Petrol., 115: 467-473.

Anonymous, 1972. Penrose field conference on ophiolite. Geotimes, 17: 24-25.

Argand E., 1911. Les nappes de recouvrement des Alpes pennines et leurs prolongements structuraux. Mat. Carte Géol. Suisse 31, 25 pp.

Barnicoat A. C. and Fry N., 1986. High pressure metamorphism of the Zermatt-Saas ophiolite Zone, Switzerland. J. Geol. Soc. London, 143: 607-618.

Bearth P., 1952. Geologie und Petrographie des Monte Rosa. Beitr. Geol. Karte Schweiz 96, 94 pp.

Bearth P., 1954. Geologischer Atlas der Schweiz 1: 25.000. Blatt Saas (Nr. 30) und Blatt Monte Moro (Nr. 31). Schweiz. Geol. Kommission.

Bearth P., 1956. Zur Geologie der Wurzelzone östlich des Ossolatales. Ecl. Geol. Helv., 49: 267-278.

Bearth P., 1957. Erläuterungen Blatt Saas und Monte Moro. Geologischer Atlas der Schweiz. Nr.30, 31. Schweiz. Geol. Kommission, Basel.

Bearth P., 1964. Geologischer Atlas der Schweiz 1:25.000. Blatt Randa (43) mit Erläuterungen. Schweiz. Geol. Kommission.

Bigioggero B., Boriani A., Colombo A. and Tunesi A., 1981. Età e caratteri petrochimici degli ortogneiss della zona Moncucco-Orselina nell'area Ossolana. Rend. Soc. It. Min. Petr., 38: 207-218.

Blumenthal M.M., 1953. Beobachtungen über Bau und Verlauf der Muldenzone von Antrona zwischen der Walliser Grenze und dem Locarnese. Ecl. Geol. Helv., 45: 219-263.

Borghi A., Compagnoni R. and Sandrone R., 1996. Composite P-T paths in the Internal Penninic Massifs of the Western Alps: Petrological constraints to their thermo-mechanical evolution. Ecl. Geol. Helv., 89: 345-367.

Bucher K., Fazis Y., De Capitani C. and Grapes R., 2005. Blueschists, eclogites, and decompression assemblages of the Zermatt-Saas ophiolite: High-pressure metamorphism of subducted Tethys lithosphere. Am. Mineral., 90: 821-835.

Carrupt E. and Schlup M., 1998. Métamorphism et téctonique du versant sud du Val Bognanco (Pennique, Alpes italiennes). Bull. Soc. Vaud. Sci. Nat., 86: 29-59.

Cartwright I. and Barnicoat A.C., 2002. Petrology, geochronology, and tectonics of shear zones in the Zermatt-Saas and Combin zones of the Western Alps. J. Metam. Geol., 20: 263-281.

Colombi A., 1989. Métamorphisme et géochimie des roches mafiques des Alpes ouest-centrales (géoprofil Viége-Domodossola-Locarno). Mém. Géol. (Lausanne), 4, 216 pp.

Colombi A. and Pfeifer H.-R., 1986. Ferrogabbroic and basaltic meta-eclogites from the Antrona mafic-ultramafic complex and the Centovalli-Locarno region (Italy and Southern Switzerland) - first results. Schweiz. Mineral. Petrogr. Mitt., 66: 99-110.

Dal Piaz G,V., 1964. Il cristallino antico del versante meridionale del Monte Rosa, paraderivati a prevalente metamorfismo alpino. Rend. Soc. Min. It., 20: 101-135.

Dal Piaz G.V., 1966. Gneiss ghiandoni, marmi ed anfiboliti antiche del ricoprimento Monte Rosa nell'alta Valle d'Ayas. Boll. Soc. Geol. It., 85: 103-132.

Dal Piaz G.V., 1993. Evolution of Austro-Alpine and Upper Penninic basement in the northwestern Alps from Variscan convergence to post-Variscan extension. In: J. Von Raumer and F. Neubauer (Eds.), Pre-Mesozoic geology in the Alps. Springer-Verlag, p. 327-344.

Dal Piaz G.V., 2001. Geology of the Monte Rosa massif: historical review and personal comments. Schweiz. Mineral. Petrogr. Mitt., 81: 275-303.

Dal Piaz G.V. and Gatto G., 1963. Considerazioni geologico-petrografiche sul versante meridionale del Monte Rosa. Rend. Acc. Naz. Lincei, Cl. Sci. Fis., 34: 190-194.

Dal Piaz G.V. and Lombardo B., 1986. Early Alpine eclogite metamorphism in the Penninic Monte Rosa-Gran Paradiso basement nappes of the north-western Alps. Geol. Soc. Am. Mem., 164: 249-265.

Ellis D.J. and Green D.H., 1979. An experimental study of the effect of Ca upon garnet-clinopyroxene Fe-Mg exchange equilibria. Contrib. Mineral. Petrol., 71: 13-22.

Ernst W.G. and Dal Piaz G.V., 1978. Mineral parageneses of eclogitic rocks and related mafic schists of the Piemonte ophiolite nappe, Breuil-St. Jacques area, Italian Western Alps. Am. Mineral., 63: 621-640.

Escher A., Masson H. and Steck A., 1987. Coupe géologique des Alpes occidentales suisses. Rapp. Géol. Serv. Hydrol. Géol. Nat. Suisse, 7.

Escher A., Masson H. and Steck A., 1993. Nappe geometry in the Western Swiss Alps. J. Struct. Geol., 15: 501-509.

Escher A., Hunziker J.C., Marthaler M., Masson H., Sartori M. and Steck A., 1997. Geologic framework and structural evolution of the western Swiss-Italian Alps. In: O.A. Pfiffner, P. Lehner, P. Heitzmann, St. Müller and A. Steck (Eds), Deep structure of the Swiss Alps. Birkäuser Verlag, Basel, p. 205-221.

Frey M., Hunziker J.C., Frank W., Bocquet J., Dal Piaz G.V., Jager E. and Niggli E., 1974. Alpine metamorphism of the Alps: a review. Schweiz. Mineral. Petrogr. Mitt., 54: 247-290.

Frey M., Hunziker J.C., O'Neil J. R. and Schwander H.W., 1976. Equilibrium-disequilibrium relations in the Monte Rosa granite, western Alps; petrological, Rb-Sr and stable isotope data. Contrib. Mineral. Petrol., 55: 147-179.

Froitzheim N., 2001. Origin of the Monte Rosa nappe in the Pennine Alps - A new working hypothesis. Geol. Soc. Am. Bull., 113: 604-614.

Fry N. and Barnicoat A.C., 1987. The tectonic implications of high-pressure metamorphism in the Western Alps. Geol. Soc. London, 144: 653-659.

Gosso G., Dal Piaz G.V., Piovano V. and Polino R., 1979. High pressure emplacement of Early-Alpine nappes, postnappe deformations and structural levels. Mem. Sci. Geol. It., 32, 15 pp.

Green T.H. and Adam J., 1991. Assessment of the garnet-clinopyroxene Fe-Mg exchange thermometer using new experimental data. J. Metam. Geol., 9: 341-347.

Heinrich W. and Althaus E., 1980. Die obere Stabilitätgrenze von Lawsonit plus Albit bzw. Jadeit. Forstchr. Mineral., 58b: 49-50.

Holland T.J.B., 1983. The experimental determination of activities in disordered and short-range ordered jadeitic pyroxenes. Contrib. Mineral. Petrol., 82: 214-220.

Hunziker J.C., 1970. Polymetamorphism in the Monte Rosa, Western Alps. Ecl. Geol. Helv., 63: 151-161.

Jaboyedoff M., Bèglè P. and Lobrinus S., 1996. Stratigraphie et évolution structurale de la zone de Furgg, au front de la nappe du Mont-Rose. Bull. Soc. Vaudoise Sci. Nat., 84: 191-210.

Kato T., 2005. New accurate Bence-Albee factors for oxides and silicates calculated from the PAP correction procedure. Geostand. Geoanal. Res., 29: 83-94.

Keller L.M. and Schmid S.M., 2001. On the kinematics of shearing near the top of the Monte Rosa nappe and the nature of the Furgg zone in val Loranco (Antrona Valley, N. Italy): tectonometamorphic and paleogeographical consequences. Schweiz. Mineral. Petrogr. Mitt., 81: 347-367.

Keller L.M., Abart R., Schmid S.M. and De Capitani C., 2005a. Phase relations and chemical compositions of phengite and paragonite in pelitic schists during decompression. A case study from the Monte Rosa Nappe and Camughera-Moncucco Unit, Western Alps. J. Petrol., 46: 2145-2166.

Keller L. M., Hess M., Fügenschuh B. and Schmid S.M., 2005b. Structural and metamorphic evolution of the Camughera-Moncucco, Antrona and Monte Rosa units southwest of the Simplon line, Western Alps. Ecl. Geol. Helv., 98: 19-49.

Kramer J., 2000. The Penninic units in the Monte Rosa region: new structural and metamorphic evidence for the provenance of the continental nappes. Abstr. 17th Swiss Tectonic Studies Group Meeting, Zürich.

Kretz R., 1983. Symbols for rock-forming minerals. Am. Mineral., 68: 277-279.

Krogh E.J., 1988. The garnet-clinopyroxene Fe-Mg geothermometer - a reintepretation of existing experimental data. Contrib. Mineral. Petrol., 99: 44-48

Laduron D., 1976. L'antiforme de Vanzone. Etude pétrographique et structurale dans la Valle Anzasca (Prov. De Novara, Italie). Ph.D. Thesis, Univ. Louvain.

Laduron D. and Merlin M., 1974. Evolution structurale et métamorphique de l'antiforme de Vanzone (Valle Anzasca, Prov. Novara, Italie). Bull. Soc. Géol. France, 16: 264-265.

Lardeaux J.M., Caron J.M., Nisio P., Pequignot G. and Boudelle M., 1986. Microstructural criteria for reliable thermometry in low-temperature eclogites. Lithos, 19: 187-203

Leake B.E., Wolley A.R., Arps C.E.S., Birch W.D., Gilbert M.C., Grice J.D., Hawthorne F.C., Kato A., Kisch H.J., Krivovichev V.G., Linthout K., Laird J., Mandarino J.A., Maresch W.V., Nickel E.H., Rock N.M.S., Schumaker J.C., Smith D.C., Stephenson N.C.N., Ungaretti L., Whitaker E.J.W. and Youzhi G., 1997. Nomenclature of amphiboles: report of the subcommittee on Amphiboles of the International Mineralogical Association, Commission on New Mineral Names. Am., Mineral., 82: 1019-1037.

Liati A., Gebauer D., Froitzheim N. and Fanning M., 2001. U-Pb SHRIMP geochronology of an amphibolitized eclogite and an orthogneiss from the Furgg zone (Western Alps) and implications for its geodynamic evolution. Schweiz. Mineral. Petrogr. Mitt., 81: 379-393.

Martin S. and Tartarotti P., 1989. Polyphase HP metamorphism in the ophiolitic glaucophanites of the lower St. Marcel Valley (Aosta, Italy). Ofioliti, 14: 135-156.

Maruyama S., Cho M. and Liou J.G., 1986. Experimental investigation of blueschist-greenschist transition equilibria: pressure dependance of Al_2O_3 contents in sodic amphiboles. A new geobarometer. Geol. Soc. Am., Spec. Issue: Blueschists and eclogites, p. 1-16.

Mercier J-C. C. and Nicolas A., 1975. Textures and fabrics of upper-mantle peridotites as illustrated by xenoliths from basalts. J. Petrol., 16: 454-487.

Michard A., Goffé B., Chopin Ch. And Henry C., 1996. Did the Western Alps develop through Oman-type stage? The geotectonic setting of high-pressure metamophism in two contrasting Tethyan transects. Ecl. Geol. Helv., 89: 43-80.

Milnes A.G., Greller M. and Müller R., 1981. Sequence and style of major post-nappe structures, Simplon-Pennine Alps. J. Struct. Geol., 3: 411-420.

Morimoto N., 1989. Nomenclature of pyroxenes. Can. Mineral., 27: 143-156.

Nicolas A. and Poirier J.-P., 1976. Crystalline plasticity and solid state flow in metamorphic rocks. Wiley, New York, 1976.

Oberhänsli R., 1980. P-T Bestimmungen anhand von Mineralanalysen in Eklogiten und Glaukophaniten der Ophiolite von Zermatt. Schweiz. Mineral. Petrogr. Mitt., 60: 215-235.

Pfeifer H.R., Colombi A. and Ganguin J., 1989. Zermatt-Saas and Antrona Zone: A petrographic and geochemical comparison of polyphase metamorphic ophiolites of the West-Central Alps. Schweiz. Mineral. Petrogr. Mitt., 69: 217-236.

Pognante U., 1989. Lawsonite, blueschsis and eclogite formation in the southern Sesia zone (western Alps, Italy). Eur. J. Mineral., 1: 89-104.

Pouchou, J. L. and F. Pichoir, 1985. r(rZ) procedure for improved quantitative microanalysis. In: J. T. Armstrong (Ed.), Microbeam analysis. San Francisco Press, Inc., San Francisco, California, USA, 104 pp.

Powell R., 1985. Regression diagnostic and robust regression in geothermometer/geobarometer calibration: the garnet-clinopyroxene geothermometer revisited. J. Metam. Geol., 3: 231-243.

Ravna E.J.K., 2000. The garnet-clinopyroxene Fe^{2+}-Mg geothermometer: an updated calibration. J. Metam. Geol., 18: 211-219.

Reinecke T., 1991. Very high pressure metamorphism and uplift of coesite-bearing metasediments from the Zermatt-Saas zone, Western Alps. Eur. J. Mineral., 3: 7-17.

Reinecke T., 1998. Prograde high- to ultrahigh-pressure metamorphism and exhumation of oceanic sediments at Lago di Cignana, Zermatt-Saas Zone, western Alps. Lithos, 42: 147-189.

Richard L.R. and Clarke D.B., 1990. AMPHIBOL: A program for calculating structural formulae and for classifying and plotting chemical analyses of amphiboles. Am. Mineral., 75: 421-423.

Spear F.S., 1993. Metamorphic phase equilibria and pressure-temperature-time paths. Min. Soc. Amer. Monogr., 799 pp.

Steck A., Epard J.L., Escher A., Lehner P., Marchant R. and Masson H., 1997. Geological interpretation of the seismic profiles through Western Switzerland: Rawil (W1)., Val d'Anniviers (W2), Matertal (W3), Zmutt-Zermatt-Findelen (W4) and Val de Bagnes (W5). In: O.A. Pfiffner, P. Lehner, P. Heitzmann, St. Müller and A. Steck (Eds), Deep structure of the Swiss Alps. Birkäuser Verlag. Basel, p. 123-137.

Steck A., Epard J. L., Escher A., Gouffon Y. and Masson H., 2001. Carte tectonique des Alpes de Suisse occidentale et des régions avoisinantes 1:100.000. Notice explicative. Office fédérale des eaux et de la géologie, 73 pp.

Turco F., 2004. Studio geologico ed evoluzione metamorfica delle ofioliti di Antrona (bassa Val Loranco, Domodossola, NE Piemonte). Unpubl. Laurea thesis, Dipart. Sci. Terra "A.Desio", Univ. Studi Milano, 138 pp.

Vernon R.H., 2004. A practical guide to rock microstructure. Cambridge Univ. Press, Cambridge U.K., 594 pp.

Wetzel R., 1972. Zur Petrographie und Mineralogie der Furgg-Zone (Monte Rosa- Decke). Schweiz. Mineral. Petrogr. Mitt., 52: 161-236.

Received, March 3, 2006
Accepted, Novembre 20, 2006